VI. PHYSICAL ACOUSTICS[*]

Prof. K. U. Ingard
Dr. L. W. Dean III
Dr. G. C. Maling, Jr.
Dr. H. L. Willke, Jr.

B. L. Chrisman
P. A. Fleury V
K. W. Gentle
G. M. Irwin
A. A. Maduemezia

W. M. Manheimer
J. H. Turner
S. D. Weiner
J. M. Witting

A. INVESTIGATION OF ULTRASONIC COUPLING AND RELAXATION EFFECTS AT A CORONA-NEUTRAL GAS INTERFACE

Our work has involved the design and assembly of a three-part system: (i) a device to generate high-frequency acoustic waves in a medium-density corona, (ii) a connecting tube in which the acoustic wave propagates from the carrier in the corona to a neutral-gas carrier, and (iii) a microphone receiving unit that picks up the sound from the neutral gas and displays its intensity and frequency on an oscilloscope. A vacuum system is provided, as well as facilities to measure pressure in the tube and to introduce inert gases.

A cross section of the tube and a block diagram of the circuit is shown in Fig. VI-1. A compact RF corona is generated between the brass ring (A) and the tungsten point (B) at one end of the tube. The RF power to the corona is then modulated at an acoustic
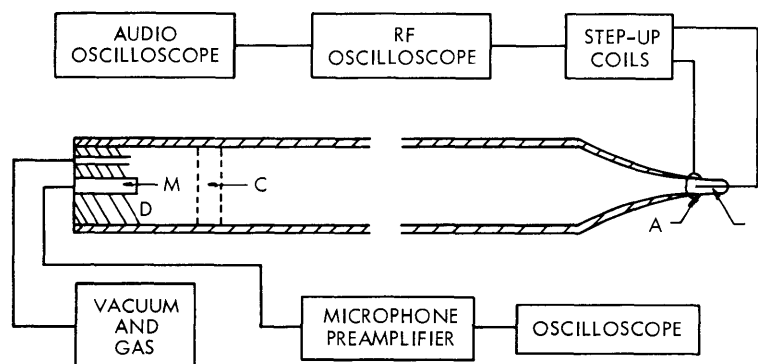

Fig. VI-1. The experimental apparatus.

frequency, and a sound wave propagates across the corona-neutral gas boundary and down the tube where it is detected by a microphone (M). Our present corona dissipates between 10 watts and 50 watts of power at an RF frequency of approximately 30 mc; we have been able to produce fairly intense sound with the device to date and are working to achieve efficiency and stability in corona power dissipation. We are also experimenting

with condenser and crystal microphones and have been forced to install RF shielding grids (C) and acoustically absorbent glass wool (D) in an attempt to minimize RF noise and standing-wave resonances at the microphone.

As soon as we have constructed a satisfactory microphone that will operate within a 0.1-2 atm range of pressures and is sufficiently sensitive at high frequencies, we plan to take some curves of sound pressure versus ambient pressure for several frequencies within the range 100 cps-50 kc. It is hoped that resonance effects observed on these plots will help us to characterize the acoustic coupling at the corona-neutral gas surface, and, specifically, to identify the parameter dependence of the time constant of relaxation at the interface.

B. L. Chrisman, G. M. Irwin

B. ACOUSTIC RADIATION FROM MOVING POINT MULTIPOLES

The fields of periodic point acoustic sources approximate those of physical sources of sufficiently small spatial extent compared with a characteristic radiation length. For moving sources, such an approximation is possible only at velocities V sufficiently small with respect to the speed of sound c, since the wavelength within the source contracts to nothing along the direction of motion as the speed of sound is approached. Moving point sources thus exhibit, at $\beta = \dfrac{V}{c} = 1$, peculiarities that are uncharacteristic of physical sources, such as the discontinuous vanishing of the fields in advance of the source and the divergence of the total radiated power from the source.

We have considered radiation from mass/heat sources of the type

$$Q^{\ell mn} = Q \cos \omega t \left(-\frac{\partial}{\partial x}\right)^{\ell} \left(-\frac{\partial}{\partial y}\right)^{m} \left(-\frac{\partial}{\partial z}\right)^{n} \delta(x-Vt)\, \delta(y)\, \delta(z). \tag{1}$$

The total acoustic power radiated by such a source can be written in the form

$$W_Q^{\ell mn} = \frac{\omega^2 Q_o^2}{8\pi\rho c} \left(\frac{\omega}{c}\right)^{2(\ell+m+n)} (2\ell)!\,(2m-1)!!\,(2n-1)!!\,(2\ell+2m+2n+3)$$

$$\cdot \left(\frac{1}{1-\beta^2}\right)^{2\ell+m+n+2} \sum_{k=0}^{\ell} \frac{1}{(2\ell-2k)!!\,(2\ell+2m+2n-2k+3)!!} \frac{\beta^{2k}}{(2k)!}. \tag{2}$$

According to (2), the radiation from an (ℓ, m, n)-pole diverges at $\beta = 1$ as $\left(\dfrac{1}{1-\beta}\right)^{2\ell+m+n+2}$, in which longitudinal multipolarity enters twice as strongly as transverse. For the lowest few orders of multipoles we have explicitly

(i) monopoles:

$$W_Q^{000} = \frac{\omega^2 Q_o^2}{8\pi\rho c} \left(\frac{1}{1-\beta^2}\right)^2$$

(ii) dipoles:

$$W_Q^{010} = W_Q^{001} = \frac{\omega^4 Q_o^2}{24\pi\rho c^3} \left(\frac{1}{1-\beta^2}\right)^3$$

$$W_Q^{100} = \frac{\omega^4 Q_o^2}{24\pi\rho c^3} \frac{1+5\beta^2}{(1-\beta^2)^4} \tag{3}$$

(iii) quadrupoles:

$$W_Q^{020} = W_Q^{002} = 3W^{011} = \frac{\omega^6 Q_o^2}{40\pi\rho c^5} \left(\frac{1}{1-\beta^2}\right)^4$$

$$W_Q^{110} = W_Q^{101} = \frac{\omega^6 Q_o^2}{120\pi\rho c^5} \frac{1+7\beta^2}{(1-\beta^2)^5}$$

$$W_Q^{200} = \frac{\omega^6 Q_o}{40\pi\rho c^5} \frac{1+14\beta^2+35\beta^4}{(1-\beta^2)^6}$$

The forcing term $-\frac{\partial F_i}{\partial x_i}$ and the Reynolds stress term $\frac{\partial^2}{\partial x_i \partial x_j}\rho v_i v_j$ in the wave equation give rise to radiation of a different character from that of the mass term $\frac{\partial Q}{\partial t}$, because of the absence of the time derivative. Following (1), we combine these remaining terms into a general forcing source

$$F^{\ell mn} = \left(-\frac{\partial}{\partial x_1}\right) F_1^{\ell-1, m, n} + \text{etc.} \tag{4}$$

The power $W_F^{\ell mn}$ radiated by the source (4) is derivable from the recursion relation

$$W_F^{\ell mn} = W_Q^{\ell-1, m, n}\bigg|_{Q_o = F/c} - \frac{2m+2n+2}{2n+1} W_F^{\ell-1, m, n+1}, \tag{5a}$$

together with the end terms

$$W_F^{0mn} = \frac{F^2}{8\pi\rho c}\left(-\frac{\omega^2}{V^2}\right)^{m+n} \frac{(2m-1)!!\,(2n-1)!!}{(2m+2n)!!}\left[\frac{1}{2\beta}\log\frac{1+\beta}{1-\beta}\right.$$

$$\left. -\frac{1}{1-\beta^2}\sum_{k=0}^{m+n-1}\frac{(2k)!!}{(2k+1)!!}\left(\frac{-\beta^2}{1-\beta^2}\right)^k\right]. \tag{5b}$$

The iterated solutions of (5) for $W_F^{\ell mn}$ are apparently too cumbersome to be of use.

Near $\beta = 1$, however, we have simply

$$W_F^{\ell mn} \approx W_Q^{\ell-1, m, n}\bigg|_{Q_o = F/c} = 0\left(\frac{1}{1-\beta^2}\right)^{2\ell+m+n} \qquad \ell > 0$$

$$W_F^{0mn} = 0\left(\frac{1}{1-\beta^2}\right)^{m+n} \qquad\qquad m+n > 0 \qquad\qquad (6)$$

$$W_F^{000} = 0\left(\frac{1}{2\beta}\log\frac{1+\beta}{1-\beta}\right).$$

According to (4), $W_F^{\ell mn}$ arises from source terms of lower multipole strength, for example, $F_1^{\ell-1, m, n}$, and W_F^{000} in particular arises not from a point monopole source but from a force whose divergence yields a point monopole, that is, a Coulomb force.

The lowest few iterates of (5) are

(i) monopoles:

$$W_F^{000} = \frac{F^2}{8\pi\rho c}\frac{1}{2\beta}\log\frac{1+\beta}{1-\beta} = \frac{F^2}{8\pi\rho c}\frac{1}{\beta}\tanh^{-1}\beta$$

representing radiation from a moving "charge";

(ii) dipoles:

$$W_F^{010} = W_F^{001} = \frac{\omega^2 F^2}{16\pi\rho c^3}\left[\frac{1}{1-\beta^2} - \frac{\tanh^{-1}\beta - \beta}{\beta^3}\right]$$

$$W_F^{100} = \frac{\omega^2 F^2}{8\pi\rho c^3}\left[\frac{\beta^2}{(1-\beta^2)^2} + \frac{\tanh^{-1}\beta - \beta}{\beta^3}\right],$$

which actually represent radiation from directed forcing monopoles;

(iii) quadrupoles:

$$W_F^{020} = W_F^{002} = 3W_F^{011} = \frac{\omega^4 F^2}{64\pi\rho c^5}\left[\frac{1+\beta^2}{(1-\beta^2)^2} + 3\frac{\tanh^{-1}\beta - \frac{\beta^3}{3} - \beta}{\beta^5}\right]$$

$$W_F^{110} = W_F^{101} = \frac{\omega^4 F^2}{16\pi\rho c^5}\left[\frac{1+\beta^4}{3(1-\beta^2)^3} - \frac{\tanh^{-1}\beta - \frac{\beta^3}{3} - \beta}{\beta^5}\right]$$

$$W_F^{200} = \frac{\omega^4 F^2}{8\pi\rho c^5}\left[\frac{6\beta^2 - \beta^4 + \beta^6}{3(1-\beta^2)^4} + \frac{\tanh^{-1}\beta - \frac{\beta^3}{3} - \beta}{\beta^5}\right]$$

representing dipole forcing terms, as well as the lowest order contributions from the Reynolds stress.

At present, we are trying to evaluate the acoustic power radiated by an extended moving source.

H. L. Willke, Jr.

C. STUDIES OF SHOCK STRUCTURE

A collisionless plasma in which an ion Larmor radius fits inside the apparatus and exceeds the Debye length is indeed difficult to obtain in the laboratory. Nevertheless, a number of theories, some of them contradictory, have been set forth for such plasma conditions. Most of the theories pertain to the structure of the collisionless shock wave.

A controversial issue being argued at present is how energy is dissipated in such shock waves. Many mechanisms are capable of dissipating enough energy. How much of the required energy is dissipated by the various mechanisms is disputed. E. N. Parker[1] proposes that mechanisms producing thin shock waves dissipate the most energy. F. J. Fishman, A. R. Kantrowitz, and H. E. Petschek[2] propose that mechanisms producing thick shock waves dissipate the most energy.

The same situation occurs in other media. In the hydraulic jump, for example, three energy-dissipation mechanisms exist. Some energy can be dissipated by radiation by
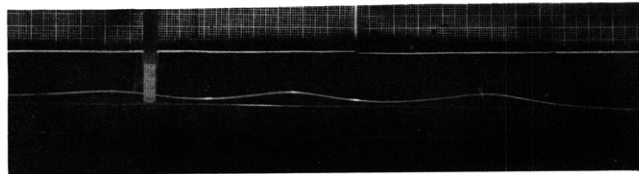

Fig. VI-2. Profile of a weak hydraulic jump, Mach 1.24, proceeding to the right. The horizontal line marks the water level before the jump is propagated. Scale, 10 divisions per 0.5 inch.
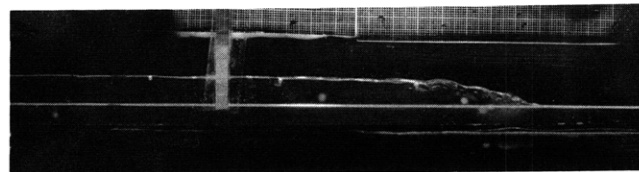

Fig. VI-3. Profile of a strong hydraulic jump, Mach 1.70, proceeding to the right. The horizontal line marks the water level before the jump is propagated. Scale, 10 divisions per 0.5 inch.

means of gravity waves behind the shock front; this produces the thickest jump. Energy can be dissipated by turbulence at the front; this produces a thinner jump. Energy can be dissipated by radiation by means of capillary waves ahead of the shock front; this produces the thinnest jump. Experimental studies of jump structure can tell which mechanisms are important and which are not. Since the arguments given by the authors mentioned above do not depend on the medium, such hydraulic jump studies apply to the "thinnest shock hypothesis" and the "thickest shock hypothesis."

Experiments on surface shock waves (hydraulic jumps) have been performed, and the observations have been the following: For weak jumps, from Mach 1 to Mach 1.25, the waves behind dissipate the bulk of the necessary energy (see Fig. VI-2). At Mach 1.25, the first wave breaks, and some energy is dissipated by turbulence. The turbulence dissipates an increasing share of the energy until, by approximately Mach 1.6, no trace of wave behind is left (see Fig. VI-3). Once the turbulence sets in, the waves behind carry much less energy than possible. Capillary waves of short wavelength are seldom observed, and those observed probably are not part of the jump structure.

Thus, the mechanism producing the thinnest jump is absent; the mechanism producing the thickest jump predominates only when turbulence is not present. Hence, Parker's hypothesis seems to be invalid, and that of Fishman, Kantrowitz, and Petschek seems to be valid if turbulence is set aside as an exception.

J. M. Witting

References

1. E. N. Parker, Astrophys. J. 129, 217 (1959).

2. F. J. Fishman, A. R. Kantrowitz, and H. E. Petschek, Revs. Modern Phys. 32, 959 (1960).